

Nearest Reversible Markov Chains with Sparsity Constraints: An Optimization Approach

Stefano Cipolla^[0000-0002-8000-4719] and
Fabio Durastante^[0000-0002-1412-8289] and
Miryam Gnazzo^[0000-0002-4381-5766] and
Beatrice Meini^[0000-0003-3139-2513]

Abstract Reversibility is a key property of Markov chains, central to algorithms such as Metropolis–Hastings and other MCMC methods. Yet many applications yield non-reversible chains, motivating the problem of approximating them by reversible ones with minimal modification. We formulate this task as a matrix nearness problem and focus on the practically relevant case of sparse transition matrices. The resulting optimization problem is a quadratic programming problem, and numerical experiments illustrate the effectiveness of the approach. This framework provides a principled way to enforce reversibility and sparsity patterns in Markov chains with applications in MCMC, computational chemistry, and data-driven modeling.

1 Introduction

Markov chains [17] are a fundamental tool in probability, statistics, and computational science. Their structural properties, i.e., the structural properties of their matrix representation, such as irreducibility, stationarity, or reversibility, play a role in both theoretical analysis and the construction of efficient algorithms. In particular, *reversibility*

Stefano Cipolla
School of Mathematical Sciences, University of Southampton, Building 54, Mathematical Sciences,
Highfield, Southampton, SO17 1BJ, UK. e-mail: s.cipolla@soton.ac.uk

Fabio Durastante
Dipartimento di Matematica, Università di Pisa, Largo Bruno Pontecorvo, 5 - 56127 Pisa, Italy e-mail:
fabio.durastante@unipi.it

Miryam Gnazzo
Istituto di Scienza e Tecnologie dell’Informazione “Alessandro Faedo”, CNR, Via G. Moruzzi, 1 -
56124 Pisa, Italy. e-mail: miryam.gnazzo@isti.cnr.it

Beatrice Meini
Dipartimento di Matematica, Università di Pisa, Largo Bruno Pontecorvo, 5 - 56127 Pisa, Italy. e-mail:
beatrice.meini@unipi.it

is especially important since it forms the objective of widely used algorithms such as Metropolis–Hastings [22, 13] and its more modern variants in Markov Chain Monte Carlo [12] (MCMC).

However, in many settings of interest, one starts from a given Markov chain that is *not* reversible. This raises the natural question of how a given Markov chain can be modified as little as possible to yield a reversible one. Indeed, this question has been addressed in [25] for the case of a general irreducible Markov chain by means of a quadratic programming approach, and in [11] via a Riemannian optimization approach [4] on a suitably defined manifold based on the multinomial manifold [9].

It is important to note that this problem is indeed motivated by applications in numerical linear algebra, where reversible chains often yield better spectral properties [29]; in MCMC, where reversibility ensures convergence to the target distribution; and in data-driven modeling, where observed transition data may be noisy and fail to satisfy the reversibility condition [28].

Formally, let $P \in \mathbb{R}^{n \times n}$ denote the transition matrix of a discrete, homogeneous Markov chain. The goal is to construct a reversible chain that is “closest” to P , in the sense of requiring the smallest possible perturbation to enforce reversibility. At the matrix level, this leads to a *matrix nearness problem* [15], of the form

$$d(P) = \min \{ \|X - P\| : X \in \mathbb{R}^{n \times n} \text{ has property } \mathfrak{P} \},$$

where \mathfrak{P} denotes a prescribed property. The value $d(P)$ then measures the minimum-norm perturbation needed to enforce the chosen property in the given matrix norm $\|\cdot\|$. In the present setting, \mathfrak{P} is the reversibility condition, expressed through the detailed balance equations

$$\pi_i X_{ij} = \pi_j X_{ji}, \quad \forall i, j,$$

with respect to a stationary distribution π , i.e., $\pi^\top X = \pi^\top$, $\pi^\top \mathbf{1} = 1$, $\pi > 0$, where $X \geq 0$, $X\mathbf{1} = \mathbf{1}$, and the distance is measured in the Frobenius norm,

$$\|A\|_F = \text{trace}(A^\top A)^{1/2}.$$

Previous work [25, 11] has focused primarily on the case where P is irreducible, and any pair of states can be connected by a nonzero transition probability. In contrast, we are interested here in the setting where the transition matrix P is *sparse*. This is the typical situation in high-dimensional applications, where each state can only transition to a small number of states. In such cases, it is natural to require that the matrix X obtained at the end preserves as much of the sparsity pattern of P as possible, so that the resulting reversible chain remains computationally efficient to simulate and analyze. To ensure reproducibility, the code for all numerical experiments supporting the proposed approach is available at the GitHub repository [Cirdans-Home/sparse-reversible](https://github.com/Cirdans-Home/sparse-reversible).

The remainder of the paper is organized as follows. In Section 1.1 we introduce the notation and basic definitions that will be used throughout the work. Section 2 formally states the problem of finding the nearest reversible Markov chain, with sparse transition matrix, and discusses feasibility and convexity issues, with particular attention to the role of reversibility constraints. In Section 3 we describe our proposed solution method based on a quadratic programming approach. Numerical experiments illustrating the

performance and properties of the approach are presented in Section 4. Finally, Section 5 summarizes the main findings and outlines directions for future research.

1.1 Notation

We begin by establishing notation and recalling the necessary background; we refer the reader to [17] for a comprehensive introduction to Markov chains, and to [3] for properties of nonnegative matrices.

A matrix $A \in \mathbb{R}^{m \times n}$ is said to be *nonnegative* (*positive*) if $A_{ij} \geq 0$ ($A_{ij} > 0$) for any i, j , and will write $A \geq 0$ ($A > 0$).

Definition 1 (Discrete-time homogeneous Markov chain) A *discrete-time homogeneous Markov chain* on a finite state space $\{1, \dots, n\}$ is a stochastic process $\{X_k\}_{k \geq 0}$ such that

$$\mathbb{P}(X_{k+1} = j \mid X_k = i, X_{k-1}, \dots, X_0) = \mathbb{P}(X_{k+1} = j \mid X_k = i) = P_{ij},$$

for all $i, j \in \{1, \dots, n\}$. The transition probabilities P_{ij} form the entries of a matrix $P = (P_{ij})$, called the *transition matrix*. The homogeneity assumption means that P does not depend on k .

Definition 2 (Stochastic matrices) A *stochastic matrix* $P \in \mathbb{R}^{n \times n}$ is a matrix such that

$$P\mathbf{1} = \mathbf{1}, \quad P \geq 0,$$

where $\mathbf{1} = (1, \dots, 1)^\top$. The transition matrices of finite-state Markov chains are stochastic matrices.

Definition 3 (Stationary distribution) Let $P \in \mathbb{R}^{n \times n}$ be the transition matrix of a Markov chain on $\{1, \dots, n\}$. A probability vector $\boldsymbol{\pi} \in \mathbb{R}^n$ with $\boldsymbol{\pi} \geq 0$, $\boldsymbol{\pi}^\top \mathbf{1} = 1$, is called a *stationary distribution* for P if

$$\boldsymbol{\pi}^\top P = \boldsymbol{\pi}^\top.$$

If the chain is *irreducible*, i.e., if for every pair of states (i, j) there exists a $k \geq 0$ such that $[P^k]_{ij} > 0$, then the Perron–Frobenius theorem [23, §8, p.667] implies that there exists a unique stationary distribution $\boldsymbol{\pi}$, the entries of $\boldsymbol{\pi}$ are strictly positive, i.e., $\pi_i > 0$ for all i , and that $\boldsymbol{\pi}$ is the unique probability vector that is a left eigenvector of P associated with the eigenvalue 1.

Definition 4 (Reversibility) A Markov chain with irreducible transition matrix P is said to be *reversible with respect to a stationary distribution $\boldsymbol{\pi}$* if the *detailed balance equations* hold:

$$\pi_i P_{ij} = \pi_j P_{ji}, \quad \forall i, j. \quad (1)$$

Equivalently, reversibility means that the probability flux between any two states is symmetric under $\boldsymbol{\pi}$.

Consider a reversible Markov chain, with stationary distribution π . Then, we may express the detailed balance equations in (1) in terms of the transition matrix P of the Markov chain. Indeed, this translates into:

$$D_\pi P = P^\top D_\pi,$$

where $D_\pi = \text{diag}(\pi_1, \dots, \pi_n)$. Note that, by performing a similarity transformation with the diagonal matrix $D_{\hat{\pi}} = \text{diag}(\hat{\pi})$, where $\hat{\pi} = \pi^{1/2}$ entrywise, we get that

$$D_\pi P = P^\top D_\pi \Leftrightarrow D_{\hat{\pi}} P D_{\hat{\pi}}^{-1} = D_{\hat{\pi}}^{-1} P^\top D_{\hat{\pi}} = (D_{\hat{\pi}} P D_{\hat{\pi}}^{-1})^\top.$$

Moreover, the stochasticity of P leads to the additional property:

$$D_{\hat{\pi}} P D_{\hat{\pi}}^{-1} \hat{\pi} = D_{\hat{\pi}} P \mathbf{1} = D_{\hat{\pi}} \mathbf{1} = \hat{\pi}.$$

The above motivates the introduction of the following set. Given a positive probability vector π we define

$$\mathcal{R}_\pi \triangleq \{S \in \mathbb{R}^{n \times n} : S \geq 0, S = S^\top, S \hat{\pi} = \hat{\pi}, \hat{\pi} = \pi^{1/2}\}, \quad (2)$$

which collects symmetric non negative matrices, with fixed eigenvector $\hat{\pi}$ associated with eigenvalue 1.

Since our main interest lies in Markov chains where each state can transition only to a limited number of other states—that is, chains whose transition matrix contains a number of nonzero entries proportional to n rather than n^2 —we introduce the following notation to describe and work with their sparsity pattern.

Definition 5 (Sparsity pattern) For any matrix $M \in \{0, 1\}^{n \times n}$ we define its sparsity pattern as

$$\Omega_M = \{(i, j) : 1 \leq i, j \leq n, M_{ij} \neq 0\}, \quad s_M = |\Omega_M|,$$

and denote by

$$\mathbb{S}(M) = \{B \in \mathbb{R}^{n \times n} : B_{ij} \neq 0 \implies (i, j) \in \Omega_M\}$$

the set of matrices that share the same sparsity pattern as M .

In this work, we refer to Markov chains whose transition matrix P is sparse as *sparse Markov chains*.

We end this section fixing a few additional notations. We will use the vec operator, which transforms a matrix into a vector by stacking its columns sequentially. A key identity involving this operator is $\text{vec}(AXB) = (B^\top \otimes A) \text{vec}(X)$, where “ \otimes ” denotes the Kronecker product and A , X , and B are matrices of compatible dimensions (with A or B possibly being vectors). This relation will be used in rewriting matrix equations as linear constraints in vector form. Finally, we denote by “ \circ ” the entry-wise or Hadamard product of two matrices. We denote by $\text{triu}(\cdot)$ the operation of extracting the upper triangular part of a matrix.

2 Formulation of the optimization problem

Consider a given Markov chain with transition matrix $P \in \mathbb{R}^{n \times n}$, a positive probability vector $\pi \in \mathbb{R}^n$ and a given irreducible matrix $M \in \{0, 1\}^{n \times n}$, which defines the sparsity pattern Ω_M . We assume that M is symmetric and $M_{ii} = 1$ for any $i = 1, \dots, n$.

We are looking for a transition matrix $X \in \mathbb{R}^{n \times n}$, which is close to the original matrix P , and is reversible with respect to the probability distribution π . Additionally, we require that the matrix X has the prescribed sparsity pattern Ω_M . Specifically, we seek a matrix $X \in \mathbb{R}^{n \times n}$ such that

$$X\mathbf{1} = \mathbf{1}, D_\pi X = X^\top D_\pi, X \geq 0, X \in \mathbb{S}(M). \quad (3)$$

This translates into solving the optimization problem

$$\begin{aligned} \min_{X \in \mathbb{R}^{n \times n}} \quad & \frac{1}{2} \|X - P\|_F^2, \\ \text{s.t. } \quad & X \text{ satisfies the relations in (3)}. \end{aligned} \quad (4)$$

The term $\|X - P\|_F^2$ measures the distance between the original matrix P and the final reversible one X . Consequently, this choice of the cost function drives the optimization procedure toward the reversible matrix closest to the original one, with respect to the distance induced by the Frobenius norm.

As a first step, rather than working directly with the set of reversible stochastic matrices sharing the stationary distribution π , we reformulate the problem in terms of the set \mathcal{R}_π defined in (2). As a consequence, we may perform the minimization in (4) choosing as feasible set the matrices in \mathcal{R}_π with pattern Ω_M .

This can be achieved performing the change of variable $Y = D_{\hat{\pi}} X D_{\hat{\pi}}^{-1}$. Indeed, since X is reversible with pattern Ω_M , we conclude that $Y \in \mathcal{R}_\pi \cap \mathbb{S}(M)$.

Then, employing this change of variables both in the objective function and in the feasible set, we construct the following optimization problem in the variable Y :

$$\begin{aligned} \min_{Y \in \mathbb{R}^{n \times n}} \quad & J(Y) := \frac{1}{2} \|D_{\hat{\pi}}^{-1} Y D_{\hat{\pi}} - P\|_F^2, \\ \text{s.t. } \quad & Y \in \mathcal{R}_\pi \cap \mathbb{S}(M). \end{aligned} \quad (5)$$

Remark 1 Observe that, by Definition 4, any reversible matrix P with stationary vector π can be rescaled, via equivalence with the matrix $D_{\hat{\pi}}$, so as to obtain an element of the set \mathcal{R}_π defined in (2). Conversely, any matrix in the set \mathcal{R}_π in (2) is such that the matrix $P = D_{\hat{\pi}}^{-1} S D_{\hat{\pi}}$ is stochastic and satisfies the detailed balance relation

$$D_\pi P = P^\top D_\pi.$$

However, P might be reducible, since S is not assumed to be irreducible, therefore P is not in general reversible according to Definition 4.

Observe that the set of matrices in \mathcal{R}_π that are irreducible is not a closed set. For example, consider the succession $R_\varepsilon \in \mathbb{R}^{n \times n}$ of stochastic reversible matrices in the form

$$R_\varepsilon = (1 - \varepsilon)I + \frac{\varepsilon}{n}\mathbf{1}\mathbf{1}^T, \quad 0 < \varepsilon \leq 1,$$

with probability distribution $\pi = \mathbf{1}/n$. For each $0 < \varepsilon \leq 1$, the matrix R_ε is irreducible. Observe that $R_\varepsilon \rightarrow I$, as $\varepsilon \rightarrow 0$. While both R_ε and I belong to the set \mathcal{R}_π , we have that the limit I is not irreducible. Therefore, to have a feasible closed set, the matrices in the set \mathcal{R}_π are not required to be irreducible.

Before solving the optimization problem in (5), we prove that, given a probability vector $\pi > 0$ and an irreducible and symmetric sparse matrix $M \in \{0, 1\}^{n \times n}$, such that $M_{ii} = 1$ for any $i = 1, \dots, n$, the feasible set

$$\{Y \in \mathbb{R}^{n \times n} : Y \in \mathcal{R}_\pi, Y \in \mathbb{S}(M)\}$$

is convex and non empty.

2.1 Constraint feasibility and convexity

Suppose we are given a probability distribution $\pi > 0$ and a prescribed pattern encoded in the irreducible matrix M ; then, we wish to construct a reversible Markov chain having π as stationary distribution and prescribed pattern Ω_{M+I} . A standard approach [5] is to construct a *proposal transition matrix* as follows. We consider the stochastic matrix $Q = D_{M\mathbf{1}}^{-1}M$. Observe that Q is an irreducible matrix in $\mathbb{S}(M + I)$, but it does not need to be reversible with respect to π and it may not even have π as its stationary distribution. Then, the idea is to correct the dynamics of Q by introducing an acceptance mechanism, yielding a new transition matrix $T = (T_{ij})_{i,j \in \{1, \dots, n\}}$ defined by

$$T_{ij} = Q_{ij} \alpha_{ij}, \quad i \neq j,$$

where $\alpha_{ij} \in [0, 1]$, for $i, j = 1, \dots, n$ is an acceptance probability. Finally, the diagonal entries are adjusted so that each row sums to one:

$$T_{ii} = 1 - \sum_{j \neq i} T_{ij}.$$

Observe that, since $\alpha_{ij} \in [0, 1]$ and Q is a stochastic matrix, we have that for $i \neq j$

$$T_{ij} = Q_{ij} \alpha_{ij} \leq Q_{ij},$$

hence

$$\sum_{j \neq i} T_{ij} \leq \sum_{j \neq i} Q_{ij} = 1 - Q_{ii}.$$

Therefore,

$$T_{ii} = 1 - \sum_{j \neq i} T_{ij} \geq 1 - (1 - Q_{ii}) = Q_{ii} \geq 0.$$

Thus every diagonal entry T_{ii} is nonnegative, and the acceptance mechanism preserves the nonnegativity of the matrix. The acceptance rule α_{ij} is then chosen to enforce the detailed balance condition

$$\pi_i Q_{ij} \alpha_{ij} = \pi_j Q_{ji} \alpha_{ji}, \quad \forall i, j \in \{1, \dots, n\}. \quad (6)$$

By construction, T is reversible with respect to π . The respect of the detailed balance condition and the row stochasticity of T imply that the constructed matrix T has as stationary distribution the vector π . As final step, we observe that the sparsity pattern of Q is directly inherited by T plus, possibly, nonzero diagonal entries. Indeed, if $Q_{ij} = 0$, then necessarily $T_{ij} = 0$, since no transition from i to j can be proposed in the first place. Moreover, the diagonal entries might be nonzero to enforce the stochasticity.

Thus, the choice of Q determines the graph of possible moves, while the acceptance rule only re-scales the allowed transitions and adds at most entries on the diagonal. Observe that we are implicitly assuming that if $Q_{ij} \neq 0$, then $Q_{ji} \neq 0$, hence the sparsity pattern of Q needs to be symmetric.

Two classical ways of choosing the acceptance probability α_{ij} are:

Metropolis rule (Metropolis–Hastings algorithm) [22, 13]: The acceptance probability is taken to be

$$\alpha_{ij} = \min\left(1, \frac{\pi_j Q_{ji}}{\pi_i Q_{ij}}\right). \quad (7)$$

Barker’s algorithm [2]: An alternative acceptance function is

$$\alpha_{ij} = \frac{\pi_j Q_{ji}}{\pi_i Q_{ij} + \pi_j Q_{ji}}.$$

Both constructions enforce reversibility of T with respect to the target distribution π , in general these are not the only closed-form constructions possible, see, e.g., [5].

The constructions above show how one may always build a reversible Markov chain with stationary distribution π , starting from an arbitrary proposal kernel Q . We can also characterize when a given transition kernel Q itself is already reversible with respect to π by means of the *Kolmogorov cycle condition* [16, Theorem 1.7]. For a Markov chain with transition matrix $T = (T_{ij})$ and stationary distribution π , reversibility holds if and only if for every finite cycle of distinct states

$$i_1 \rightarrow i_2 \rightarrow \dots \rightarrow i_k \rightarrow i_1,$$

the following equality is satisfied:

$$T_{i_1 i_2} T_{i_2 i_3} \dots T_{i_{k-1} i_k} T_{i_k i_1} = T_{i_1 i_k} T_{i_k i_{k-1}} \dots T_{i_3 i_2} T_{i_2 i_1}.$$

Equivalently, one can state the condition in terms of the stationary distribution:

$$\pi_{i_1} T_{i_1 i_2} \pi_{i_2} T_{i_2 i_3} \dots \pi_{i_k} T_{i_k i_1} = \pi_{i_1} T_{i_1 i_k} \pi_{i_k} T_{i_k i_{k-1}} \dots \pi_{i_2} T_{i_2 i_1}.$$

When the cycle condition holds, detailed balance is satisfied, and the chain is reversible with respect to π . If the cycle condition fails for even one cycle, the chain is inherently non-reversible, and one can resort to a construction such as Metropolis–Hastings, Barker or other systematic approaches [5] to enforce reversibility. We stress that the Kolmogorov cycle condition depends only on the transition structure of T , hence if T is non-reversible, it *cannot be modified locally* to restore reversibility without changing its transition graph. In contrast, by introducing a proposal kernel Q and an acceptance rule, one can always build a new reversible chain, though the resulting dynamics may differ significantly from those of the original Q and have added some diagonal entries to the transition matrix.

Following the idea in [10, Proposition 2.3] and the previous insights, we may prove that the set of admissible perturbations Δ is not empty.

Proposition 1 *Consider a probability distribution $\pi > 0$, and a pattern taken from a given irreducible matrix $M \in \{0, 1\}^{n \times n}$. Assume that M is symmetric and $M_{ii} = 1$ for any $i = 1, \dots, n$. Then, the set of matrices Y such that $Y \in \mathcal{R}_\pi$ as in (2) and $Y \in \mathbb{S}(M)$ is not empty.*

Proof. By either the Metropolis–Hastings or the Barker algorithms we know that there exist stochastic matrix $Q \in \mathbb{S}(M)$, and weighting matrix α such that the detailed balance conditions for $S = Q \circ \alpha$ hold, i.e., for which we have $S\mathbf{1} = \mathbf{1}$, and $D_\pi S = S^\top D_\pi$. In addition, we have $S \in \mathbb{S}(M)$. Scaling by the diagonal matrix $D_{\hat{\pi}}$ from both sides, we get that $D_{\hat{\pi}} S D_{\hat{\pi}}^{-1} \in \mathcal{R}_\pi$, and this scaling preserves the pattern $\mathbb{S}(M)$. Therefore, we can choose the matrix Y as $D_{\hat{\pi}} S D_{\hat{\pi}}^{-1}$. \square

Proposition 2 *Consider a probability distribution $\pi > 0$, and a pattern taken from a given irreducible matrix $M \in \{0, 1\}^{n \times n}$. Assume that M is symmetric and $M_{ii} = 1$ for any $i = 1, \dots, n$. Then, the intersection $\mathcal{R}_\pi \cap \mathbb{S}(M)$ is a convex set.*

Proof. Let Y_1 and Y_2 be two matrices in $\mathcal{R}_\pi \cap \mathbb{S}(M)$. By the definition of set \mathcal{R}_π in (2), this implies that Y_i is nonnegative, symmetric, and preserves $\hat{\pi}$, i.e., for $i = 1, 2$

$$Y_i \geq 0, Y_i = Y_i^\top, \text{ and } Y_i \hat{\pi} = \hat{\pi}.$$

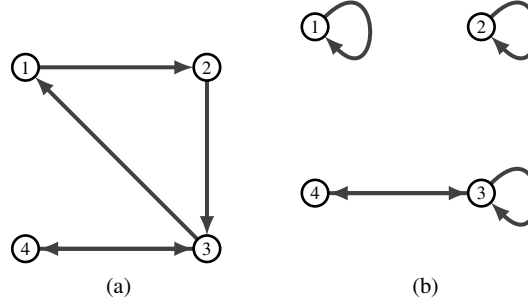
Consider a convex combination $Y_\lambda = \lambda Y_1 + (1 - \lambda) Y_2$ with $\lambda \in [0, 1]$. Y_λ is clearly nonnegative since the set of nonnegative matrices is convex. Moreover, the symmetry is preserved, since

$$(Y_\lambda)^\top = \lambda Y_1^\top + (1 - \lambda) Y_2^\top = Y_\lambda.$$

Finally, $Y_\lambda \hat{\pi} = \lambda Y_1 \hat{\pi} + (1 - \lambda) Y_2 \hat{\pi} = \hat{\pi}$, showing that $\hat{\pi}$ is an eigenvector associated with 1 for the convex combination Y_λ . Therefore, $Y_\lambda \in \mathcal{R}_\pi$ for all $\lambda \in [0, 1]$. Finally, we observe that the pattern is preserved, since $Y_1, Y_2 \in \mathbb{S}(M)$ implies $Y_\lambda \in \mathbb{S}(M)$. We then conclude that the feasible set in the optimization problem (5) is convex. \square

This implies that the matrix nearness problem with respect to Frobenius norm $\|\cdot\|_F$ admits a unique solution, as it reduces to the minimization of a strictly convex quadratic objective function over a convex feasible set. This is consistent with the behavior observed in the unstructured case studied in [11, 25].

Fig. 1 Effect of the Metropolis–Hastings adjustment on a non-symmetric stochastic matrix. The Markov chain represented by the graph in panel **1a** is irreducible, i.e., the underlying directed graph is strongly connected. On the other hand, its *reversibilization* obtained through the Metropolis–Hastings approach in panel **1b** is reducible, and the corresponding graph is made of three connected components.



Remark 2 When the Metropolis–Hastings, or equivalently Barker’s, procedure is applied to a Markov chain with a non-symmetric sparsity pattern, the resulting transition matrix may have a different support than the original one. In particular, if $T_{ij} > 0$ but $T_{ji} = 0$, then the detailed balance condition cannot be satisfied, and the Metropolis–Hastings construction sets both T_{ij} and T_{ji} equal to zero. As a consequence, all non-reciprocated transitions are eliminated, leaving only those edges of the graph that appear in both directions. In graph-theoretic terms, this means that the transition structure after the Metropolis–Hastings adjustment corresponds to the largest symmetric subgraph contained in the original directed graph. Consider, e.g., the stochastic 4×4 matrix

$$T = \begin{bmatrix} 0 & 1 & 0 & 0 \\ 0 & 0 & 1 & 0 \\ 1/2 & 0 & 0 & 1/2 \\ 0 & 0 & 1 & 0 \end{bmatrix}.$$

The corresponding directed graph is shown in Fig. **1a**. Applying the Metropolis–Hastings adjustment eliminates the one-way transitions $1 \rightarrow 2$ and $2 \rightarrow 3$, since their reciprocals do not exist, but preserves the bidirectional link between states 3 and 4. The resulting adjusted transition matrix has the symmetric support

$$\tilde{T} = \begin{bmatrix} 1 & 0 & 0 & 0 \\ 0 & 1 & 0 & 0 \\ 0 & 0 & 1/2 & 1/2 \\ 0 & 0 & 1 & 0 \end{bmatrix},$$

and its associated graph is shown in Fig. **1b**. This has the effect of also changing the structure of the associated Markov chain, which can then become reducible as in the example.

Furthermore, we remark that the direct use of the Metropolis–Hastings approach, or similar ones, does not allow to control any norm of the perturbation applied to the starting matrix, since it only performs a reversibilization of a given Markov chain,

without any theoretical guarantees on the closeness from the original one; see Fig. 4 in Section 4 for an example of this.

3 Reformulation of the optimization problem

A first reformulation of problem (5) is obtained by vectorizing both the objective function and the constraints. In the following lemma, we provide the main constructive steps behind this process.

Lemma 1 *Consider a probability vector $\boldsymbol{\pi} > 0$, and a sparsity pattern Ω_M , where $M \in \{0, 1\}^{n \times n}$ is irreducible, symmetric and such that $M_{ii} = 1$ for any $i = 1, \dots, n$. Then, the set of constraints in (5) for the matrix $Y \in \mathbb{R}^{n \times n}$ can be rephrased as a set of constraints on $\text{vec}(Y)$ as follows:*

$$\begin{aligned} (\hat{\boldsymbol{\pi}}^\top \otimes I) \text{vec}(Y) &= \hat{\boldsymbol{\pi}}, \\ (I_{n^2} - K) \text{vec}(Y) &= 0, \\ \text{diag}(\text{vec}(\mathbf{1}\mathbf{1}^\top - M \circ \mathbf{1}\mathbf{1}^\top)) \text{vec}(Y) &= 0, \\ \text{vec}(Y) &\geq 0, \end{aligned} \tag{8}$$

where K is the orthogonal commutation matrix such that $K \text{vec}(\Delta) = \text{vec}(\Delta^\top)$.

Proof. The first constraint in (8) arises from the eigenvector relation $Y\hat{\boldsymbol{\pi}} = \hat{\boldsymbol{\pi}}$, using the relation

$$\text{vec}(Y\hat{\boldsymbol{\pi}}) = (\hat{\boldsymbol{\pi}}^\top \otimes I) \text{vec}(Y).$$

The second constraint arises from the relation $Y^\top = Y$; indeed, vectorizing we get

$$(I \otimes I - (I \otimes I)K) \text{vec}(Y) = (I_{n^2} - K) \text{vec}(Y) = 0,$$

where we employed the relation $\text{vec}(Y) = (I \otimes I) \text{vec}(Y)$ and $\text{vec}(Y^\top) = K \text{vec}(Y)$.

The third constraint models the relation associated with the pattern Ω_M . In practice, we are imposing that for the entries $(i, j) \notin \Omega_M$, the corresponding element $Y_{ij} = 0$. This translates as a constraint on $\text{vec}(Y)$, imposing that

$$\text{diag}(\text{vec}(\mathbf{1}\mathbf{1}^\top - M \circ \mathbf{1}\mathbf{1}^\top)) \text{vec}(Y) = 0.$$

Lastly, the constraint on the nonnegativity of Y can be obtained performing a vectorization step. \square

As a result of the above discussion, vectorizing the objective function and taking into account all the constraints in Lemma 1, we obtain from the optimization problem in (5):

$$\begin{aligned}
\min_{Y \in \mathbb{R}^{n \times n}} J(Y) &= \frac{1}{2} \|(D_{\hat{\pi}} \otimes D_{\hat{\pi}}^{-1}) \text{vec}(Y) - \text{vec}(P)\|_2^2, \\
\text{s.t. } &(\hat{\pi}^\top \otimes I) \text{vec}(Y) = \hat{\pi}, \\
&(I_{n^2} - K) \text{vec}(Y) = 0, \\
&\text{diag}(\text{vec}(\mathbf{1}\mathbf{1}^\top - M \circ \mathbf{1}\mathbf{1}^\top)) \text{vec}(Y) = 0, \\
&\text{vec}(Y) \geq 0.
\end{aligned} \tag{9}$$

Recall that M is assumed to be symmetric and to contain the diagonal, and let s_M denote the cardinality of the pattern $\mathbb{S}(M)$. By exploiting the symmetric structure of \mathcal{R}_π , problem (5) admits a more compact reformulation than (9), in terms of both the number of variables and constraints. To this end, we observe that any matrix $Y \in \mathbb{S}(M)$ satisfying the symmetry constraint $Y = Y^\top$ can be expressed as

$$Y = M \circ \begin{bmatrix} Y_{11} & Y_{12} & \cdots & \cdots & Y_{1n} \\ Y_{12} & \ddots & \ddots & & \vdots \\ \vdots & \ddots & \ddots & \ddots & \vdots \\ \vdots & & \ddots & \ddots & Y_{(n-1)n} \\ Y_{1n} & \cdots & \cdots & Y_{(n-1)n} & Y_{nn} \end{bmatrix}. \tag{10}$$

In other words, the entries in the strictly lower triangular part are uniquely determined by the nonzero ones in the upper triangular part.

Hence, we may reformulate the optimization problem in terms of only those variables allowed to be nonzero, corresponding to the sparsity pattern of the upper triangular part $\mathbb{S}(M)$.

To this aim, let $y_M = (s_M - n)/2 + n$, with $n \leq y_M \leq s_M$, and define the vector

$$\mathbf{y} = [Y_{i_1 j_1} \ Y_{i_2 j_2} \ \cdots \ Y_{i_{y_M} j_{y_M}}]^\top,$$

where each pair $(i_k, j_k) \in \Omega_{\text{triu}(M)}$.

We start defining an operator mapping the vector \mathbf{y} into the upper triangular part of Y . To this end, define the matrix constructor $S(\mathbf{y}) \in \mathbb{R}^{n \times n}$ defined elementwise as

$$(S(\mathbf{y}))_{ij} = \begin{cases} Y_{ij}, & (i, j) \in \Omega_{\text{triu}(M)}, i < j, \\ \frac{1}{2} Y_{ii}, & i = j, \\ 0, & \text{otherwise.} \end{cases} \tag{11}$$

We have, hence, $Y = S(\mathbf{y}) + S(\mathbf{y})^\top$ and $\text{vec}(Y) = \text{vec}(S(\mathbf{y})) + K \text{vec}(S(\mathbf{y}))$. Let us now define by $r(i, j) = (j - 1)n + i$ the row index corresponding to entry (i, j) in the vectorization in $\text{vec}(S(\mathbf{y}))$ and by $k(i, j)$ the index of Y_{ij} in \mathbf{y} whenever $(i, j) \in \Omega_{\text{triu}(M)}$.

With these definitions, we can consider the operator $\Pi \in \{0, 1\}^{n^2 \times y_M}$ as

$$\Pi_{r(i,j),k} = \begin{cases} 1, & (i,j) \in \Omega_{\text{triu}(M)}, i < j, k = k(i,j), \\ \frac{1}{2}, & i = j, k = k(i,j), \\ 0, & \text{otherwise,} \end{cases} \quad (12)$$

i.e., $\Pi \mathbf{y} = \text{vec}(S(\mathbf{y}))$. Moreover, defining the weighting vector $\mathbf{d} \in \mathbb{R}^{y_M}$ with

$$d_k = \begin{cases} 1, & (i,j) \in \Omega_{\text{triu}(M)}, i < j, k = k(i,j), \\ \frac{1}{2}, & i = j, k = k(i,j), \end{cases}$$

we have

$$\Pi^\top (\Pi \mathbf{y} + K \Pi \mathbf{y}) = \Pi^\top (\text{vec}(S(\mathbf{y})) + \text{vec}(S(\mathbf{y})^\top)) = \text{diag}(\mathbf{d}) \mathbf{y},$$

where we used $\Pi^\top \text{vec}(L) = 0$ for any strictly lower triangular matrix L . Using the observations carried out until now, we find

$$\text{vec}(Y) = (I + K) \Pi \mathbf{y}.$$

Defining now, for the sake of brevity $\mathbf{p} = \text{vec}(P)$, we write (9) as

$$\begin{aligned} \min_{\mathbf{y} \in \mathbb{R}^{y_M}} \quad & \frac{1}{2} \|(D_{\hat{\pi}} \otimes D_{\hat{\pi}}^{-1})(I + K) \Pi \mathbf{y} - \mathbf{p}\|_2^2, \\ \text{s.t.} \quad & (\hat{\pi}^\top \otimes I)(I + K) \Pi \mathbf{y} = \hat{\pi} \\ & \mathbf{y} \geq 0, \end{aligned} \quad (13)$$

where we used the fact that $\Pi^\top ((I + K) \Pi \mathbf{y}) = \text{diag}(\mathbf{d}) \mathbf{y}$. It is important to note that in this formulation, we have n equality constraints and y_M variables with $n \leq y_M$, which significantly reduces the dimensionality of the problem while preserving its essential structure. Finally, it is important to note that, thanks to the following Proposition 3, the objective in (13) is strongly convex.

Proposition 3 *Given $\mathbb{R}^n \ni \pi > 0$, $K \in \mathbb{R}^{n^2 \times n^2}$ the commutation matrix for which $\text{vec}(Y^\top) = K \text{vec}(Y)$ for any $Y \in \mathbb{R}^{n \times n}$, and the projector $\Pi \in \mathbb{R}^{n^2 \times y_M}$ in (12) built from $M \in \{0, 1\}^n$ irreducible, symmetric, and with $M_{i,i} = 1$, $i = 1, \dots, n$, then*

$$\text{rank} \left((D_{\hat{\pi}} \otimes D_{\hat{\pi}}^{-1})(I + K) \Pi \right) = y_M.$$

Proof. The matrix $(D_{\hat{\pi}} \otimes D_{\hat{\pi}}^{-1})$ is a diagonal matrix of size $n^2 \times n^2$ whose diagonal entries are $\hat{\pi}_i / \hat{\pi}_j = \sqrt{\pi_i} / \sqrt{\pi_j} > 0$, $\forall i, j = 1, \dots, n$, since $\pi > 0$. Moreover, given $\mathbf{y} = \text{vec}(Y)$, it holds $(I + K) \mathbf{y} = 0$ iff $Y = -Y^\top$. Hence, to prove the thesis, we need to verify only that no vectorization of a skew-symmetric matrix is in the image of Π , since Π has full rank y_M by construction. On the other hand, this holds by construction since $\Pi \mathbf{y} = \text{vec}(S(\mathbf{y}))$ for $S(\cdot)$ the operator in (11), which returns a triangular matrix. The thesis follows by observing that the only skew-symmetric triangular matrix is the zero matrix. \square

3.1 Formulation in QP Standard form

Quadratic programming (QP) provides a natural computational framework for the reversibilization problem formulated in the previous section. We seek a matrix $X \in \mathbb{R}^{n \times n}$, endowed with the prescribed sparsity pattern Ω_M , that minimizes the Frobenius distance to the original transition matrix P while satisfying the linear constraints of reversibility, stationarity, and stochasticity. Note that the objective function $J(Y)$ is strongly convex (cf. Proposition 3) and therefore the program admits a unique solution.

For implementation with off-the-shelf solvers, it is sufficient to recognize that problem (13) can be easily cast in the standard QP form

$$\begin{aligned} \min_{\mathbf{y} \in \mathbb{R}^{yM}} \quad & \frac{1}{2} \mathbf{y}^\top Q \mathbf{y} + \mathbf{c}^\top \mathbf{y} \\ \text{subject to} \quad & A_{\text{eq}} \mathbf{y} = \mathbf{b}_{\text{eq}}, \\ & \mathbf{y} \geq 0 \end{aligned} \tag{14}$$

where $Q = ((D_{\hat{\pi}} \otimes D_{\hat{\pi}}^{-1})(I + K)\Pi)^\top (D_{\hat{\pi}} \otimes D_{\hat{\pi}}^{-1})(I + K)\Pi \in \mathbb{R}^{yM \times yM}$ is a symmetric matrix defining the quadratic part of the objective,

$$\mathbf{c}^\top = -\mathbf{p}^\top (D_{\hat{\pi}} \otimes D_{\hat{\pi}}^{-1})(I + K)\Pi \in \mathbb{R}^{yM}$$

defines the linear part, whereas $A_{\text{eq}} = (\hat{\pi}^\top \otimes I)(I + K)\Pi$ and $\mathbf{b}_{\text{eq}} = \hat{\pi}$. Hence, Proposition 3, implies that Q is positive definite and therefore the problem is strongly convex.

To solve (14) we employ two widely used solvers: MATLAB's `quadprog` and the `gurobi` QP solver. The former offers a simple interface and robust defaults suitable for prototyping and medium-scale instances; the latter provides a state-of-the-art engine with advanced presolve and parallel execution, which we found to deliver shorter runtimes on larger cases. Since the objective is strongly convex, the optimal solution is unique and therefore independent of the choice of algorithm, up to numerical precision.

3.2 The case of reducible Markov chains

As pointed out in Definition 4 and Remark 1, in Section 2 we provide a formulation limited to case of irreducible Markov chains. Nevertheless, more generally, a Markov chain may exhibit more than one ergodic class. We recall that an *ergodic class* is a subset $C \subseteq \mathcal{V}$ of the state space with the three following properties: *i*) closed, i.e. if $i \in C$ and $p_{ij} > 0$, then $j \in C$; *ii*) irreducible, that is for $i, j \in C$, there exists ℓ such that $[P^\ell]_{ij} > 0$; *iii*) aperiodic, which means that for $i \in C$, the $\text{gcd} \{ \ell \geq 1 : [P^\ell]_{ii} > 0 \} = 1$.

A Markov chain with a single ergodic class has a unique stationary distribution π , and if there are no transient states, then π is strictly positive, consistent with Definition 3. On the other hand, if the chain contains multiple ergodic classes and possibly some transient states, then the limiting behavior depends on the initial condition. In this case,

the set of stationary distributions is not a singleton but rather a convex polytope spanned by the stationary distributions of the individual ergodic classes. More concretely, after a suitable permutation of states, the transition matrix P can be expressed in block form as

$$P = \begin{bmatrix} P_1 & 0 & 0 & \cdots & 0 \\ 0 & P_2 & 0 & \cdots & 0 \\ \vdots & \ddots & \ddots & \ddots & \vdots \\ 0 & \cdots & 0 & P_E & 0 \\ P_{T1} & P_{T2} & \cdots & P_{TE} & P_{TT} \end{bmatrix}, \quad (15)$$

where each P_i is a stochastic irreducible block associated with an ergodic class, and T indexes the (possibly empty) set of transient states. In this case, every stationary distribution has the form

$$\boldsymbol{\pi}^\top = [\alpha_1 \boldsymbol{\pi}_1^\top, \dots, \alpha_E \boldsymbol{\pi}_E^\top, \mathbf{0}_{|T|}^\top], \quad (16)$$

where $\alpha_i \in [0, 1]$ with $\sum_{i=1}^E \alpha_i = 1$, each $\boldsymbol{\pi}_i$ is the unique stationary distribution of P_i , and $\mathbf{0}_{|T|}$ is the zero vector corresponding to the transient states. Hence, uniqueness and positivity of the stationary distribution are guaranteed only when $E = 1$ and $T = \emptyset$.

From the perspective of reversibility, the decomposition (15) highlights that detailed balance condition in Definition 4 can hold within the support of a stationary distribution, that is $\text{supp}(\boldsymbol{\pi}) = \{i : \pi_i > 0\}$, while for the indices corresponding to the transient states we find

$$\underbrace{\pi_i}_{=0} P_{ij} = \underbrace{\pi_j P_{ji}}_{=0}, \quad \forall i \in T, j = 1, \dots, n,$$

and since both π_i and P_{ji} are zero for any $i \in T$, these equations are automatically satisfied. If $E = 1$, reversibility is defined with respect to the unique strictly positive $\boldsymbol{\pi}$, as in Definition 4. If $E > 1$, reversibility may still hold within each ergodic block P_i with respect to its stationary distribution $\boldsymbol{\pi}_i$, but a global notion of reversibility for the entire chain requires specifying a convex combination as in (16). In this sense, reversibility is inherently a property of ergodic classes and extends to the whole chain only relative to a chosen positive stationary distribution.

This analysis suggests that, in the general case, the appropriate approach to finding the closest reversible chain with a prescribed sparsity pattern is to remove the transient states and to restrict attention to the ergodic classes. The problem can then be solved independently within each ergodic class, where the stationary distribution is strictly positive, and reversibility is well defined. An analogous treatment in the setting of dense transition matrices, where the nearest reversible chain is computed via Riemannian optimization, is given in [11, §3.2]. To identify the transient states, we compute a stationary distribution $\boldsymbol{\pi}$ as $\boldsymbol{\pi}^\top = \lim_{k \rightarrow \infty} \boldsymbol{\pi}^{(0)\top} P^k$, where $\boldsymbol{\pi}^{(0)} > 0$ is a probability vector representing the probability distribution at time 0. If P is reducible, the vector $\boldsymbol{\pi}$ depends on the initial distribution $\boldsymbol{\pi}^{(0)}$, but the indices corresponding to the zero entries of $\boldsymbol{\pi}$ uniquely identify the transient states. We describe the algorithmic approach based on this idea in Section 3.3.

3.3 The overall algorithm

In light of Section 3.2, we first decompose the chain into ergodic classes and transient states via standard graph algorithms (e.g., Tarjan’s method [27]; see also [8]). We then restrict the optimization to the support of the stationary distribution, discarding transient states since they do not affect the detailed balance condition. This reduction yields independent subproblems on the ergodic classes, each of them well-posed (Proposition 1) with a convex feasible set (Proposition 2). Problem (4) is a convex optimization problem with a strongly convex objective function and therefore admits a unique solution.

We summarize the entire strategy to obtain a sparse reversible Markov chain using the matrix nearness criterion in Algorithm 1.

<p>Input: $P \in \mathbb{R}^{n \times n}$ stochastic Output: $R \in \mathbb{R}^{n \times n}$ stochastic, reversible, sharing the stationary distribution of P, minimizing $\frac{1}{2} \ P - R\ _F^2$</p> <ol style="list-style-type: none"> 1 Compute $\pi^\top = \lim_{k \rightarrow \infty} \pi^{(0)\top} P^k$, where $\pi^{(0)} > 0$, $\pi^{(0)\top} \mathbf{1} = \mathbf{1}$; 2 Identify $\text{supp}(\pi)$ and restrict P and π to \tilde{P} and $\tilde{\pi}$, discarding transient states; 3 Identify the number of ergodic classes E of \tilde{P} via Tarjan’s depth-first search method [27]; 4 for each ergodic class C from 1 to E do 5 /* Denote by $\tilde{P} _C$ and $\tilde{\pi} _C$ the restrictions to the current ergodic class */ 6 Build $D_{\tilde{\pi}} = \text{diag}(\sqrt{\tilde{\pi} _C})$; 7 Define $\hat{P} = D_{\tilde{\pi}} \tilde{P} _C D_{\tilde{\pi}}^{-1}$; 8 Build the binary matrix $M \in \mathbb{S}(\hat{P} + \hat{P}^\top + I)$; 9 Solve the optimization problem (13) for \mathbf{y}; 10 Assemble $Y _C$ having the same pattern of M and entries obtained from \mathbf{y}; 11 $R _C = D_{\tilde{\pi}}^{-1} Y _C D_{\tilde{\pi}}$; 12 end 13 Assemble \tilde{R} by collecting $R _C$ for the E ergodic classes; 14 Reinsert the rows and columns corresponding to the zero entries of π into \tilde{R} to obtain R in the original ordering; 15 The perturbation matrix Δ is then given by $\Delta = R - P$;

Algorithm 1: Nearest reversible sparse Markov chain

It is important to note that the reduction to ergodic classes makes computations independent across classes, so the loop at Line 4 of Algorithm 1 is embarrassingly parallel. To balance load across computing units, classes can be grouped so that their total number of unknowns is approximately uniform.

The procedure in Algorithm 1 is implemented by the MATLAB function `nearest_sparse_reversible.m` in the repository [Cirdans-Home/sparse-reversible](#). Given a possibly non-reversible transition matrix P , it parses options, computes (or accepts) the stationary distribution, the pattern, and delegates the optimization to one of the available QP solvers (`'quadprog'`, `'gurobi'`). When `recurse_ergodic` is enabled, the state space is decomposed as in Section 3.2 and each ergodic block is processed independently before reassembling the global reversible chain. The outputs comprise the reversible

approximation R and an auxiliary output structure with solver diagnostics, perturbation statistics, and timings.

4 Numerical examples

This section presents a set of numerical experiments designed to assess the performance and effectiveness of the algorithm introduced in Section 3.3. The discussion is organized into two parts. The first part (Section 4.1) focuses on synthetic, sparse Markov chains of increasing dimension, with the goal of validating the proposed method across a broad class of controlled test problems. The second part (Section 4.2) examines two real-world case studies drawn from molecular dynamics. In both cases, a discrete Markov chain is estimated from simulation data to describe transitions between the various spatial conformations of a complex molecule. Although the underlying physical process is time-reversible, the estimated transition matrices are generally not reversible due to statistical and sampling errors, and therefore must be post-processed to obtain a reversible approximation.

All numerical experiments presented in this section were performed on a laptop equipped with an Intel® Core™ i9-14900HX processor (24 cores, 32 hardware threads) and 64 GB of RAM. The operating system is Ubuntu 24.04.2 LTS, and all computations were carried out using MATLAB R2025b. The MATLAB interface of version Gurobi 12.0.1 has been used.

All numerical experiments presented in this work are fully reproducible using the code available at the GitHub repository [Cirdans-Home/sparse-reversible](https://github.com/Cirdans-Home/sparse-reversible).

4.1 Benchmarking the QP approaches

In this section, we compare different solution methods for the QP problem arising from the computation of the reversible matrix closest to a given stochastic one. Specifically, we compare MATLAB’s `quadprog` solver [1], and the commercial `gurobi` QP solver¹.

4.1.1 Generation of Sparse Random Markov Chains

To evaluate the proposed methods, we construct a collection of sparse, non-reversible Markov chains with randomly varying state-space sizes. All experiments are reproducible by fixing the random seed.

Specifically, we generate $N = 100$ independent test cases. For each test case, the number of states n is drawn uniformly at random from the interval $[n_{\min}, n_{\max}]$, with $n_{\min} = 100$ and $n_{\max} = 300$. A sparse random matrix $P \in \mathbb{R}^{n \times n}$ is then constructed by sampling $\text{nnz}(P) = \lfloor \alpha n \rfloor$ nonzero entries at uniformly random positions, where $\alpha = 5$

¹ See the website www.gurobi.com to get the solver along with an academic license.

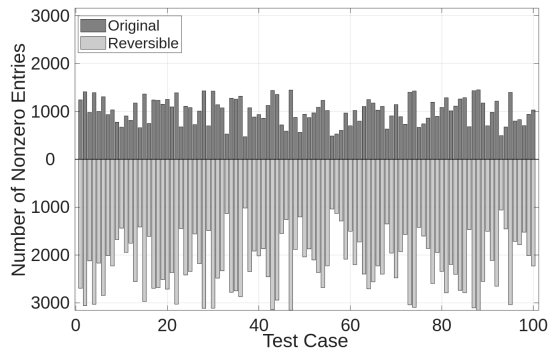
controls the sparsity level. The resulting matrix is therefore sparse, with an average of $O(n)$ nonzero entries. To ensure that the associated Markov chain is irreducible, we interpret the nonzero pattern of P as the adjacency matrix of a directed graph. We compute the strongly connected components of this graph and restrict P to the largest strongly connected component, thereby guaranteeing irreducibility of the resulting transition structure. Finally, the matrix is row-normalized to obtain a valid transition matrix,

$$\tilde{P}_{ij} = \frac{P_{ij}}{\sum_k P_{ik}}, \quad i = 1, \dots, n,$$

ensuring that each row sums to one. The resulting matrix \tilde{P} defines a sparse, irreducible, and generally non-reversible Markov chain. This procedure is repeated independently for each test case.

We apply the proposed optimization framework to compute the nearest sparse reversible Markov chain using two different optimization algorithms. We begin by reporting, in Fig. 2, a comparison between the number of nonzero entries of the original

Fig. 2 Diverging bar plots showing the number of nonzero entries in the original Markov chain (positive values) and in the recovered reversible matrix (negative values). Since the underlying optimization problem is *strongly convex*, the resulting sparsity pattern is independent of the optimization algorithm employed.



sparse transition matrix of the Markov chain and those of the corresponding reversible matrix. The reversible matrices consistently exhibit a substantially larger number of nonzero entries than their original counterparts. This behavior is expected, as enforcing reversibility introduces additional coupling constraints between forward and backward transitions, which generally leads to a denser sparsity pattern; see again Proposition 2. While the size of the original matrices varies significantly across test cases—reflecting the randomized construction—the relative increase in the number of nonzero entries remains systematic and stable. This indicates that the sparsity–reversibility trade-off is largely independent of the specific realization and is instead an intrinsic consequence of the reversibility constraint.

In Fig. 3 we report the algorithmic performances of the procedure with respect to the different optimization methods used inside. These are boxplots summarizing the empirical distribution of the reported quantities—solution times, distance to reversibility, being π the stationary distribution, and being stochastic—across all test cases for each solver. For a given method, the central line of the box denotes the median value, while the lower and upper edges of the box correspond to the first and third quartiles, respectively.

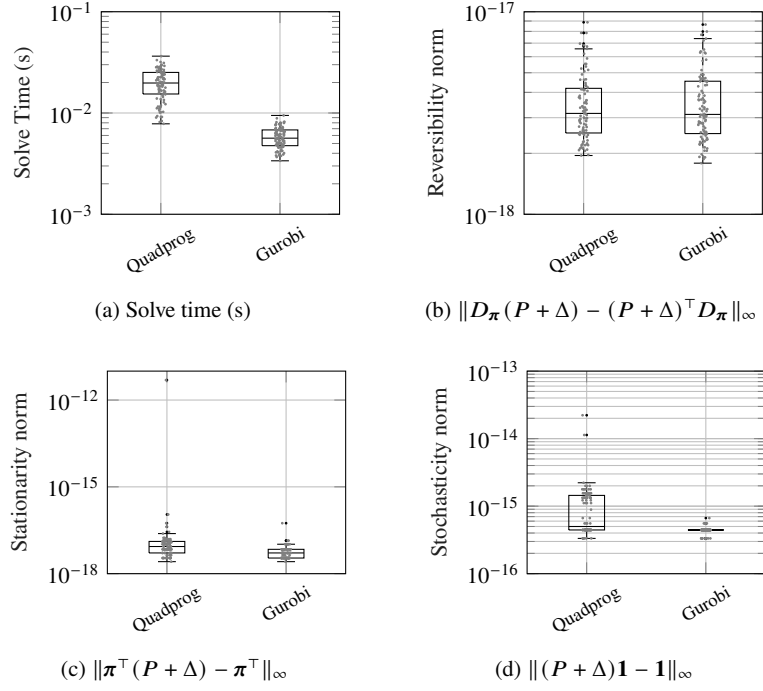
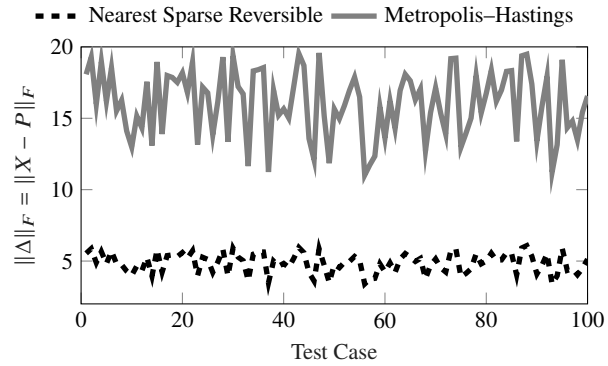


Fig. 3: Boxplots summarizing the distribution of solution times and condition numbers across all test cases, grouped by solver. Each boxplot displays the median and interquartile range, with individual test cases shown as jittered dots.

Fig. 4 Comparison of the norm of the perturbation $\Delta = X - P$ between the X obtained from P by applying Metropolis–Hastings reversibilization in (6)-(7), and the nearest-sparse reversible obtained via our optimization procedure as in Algorithm 1 while employing the gurobi QP solver.

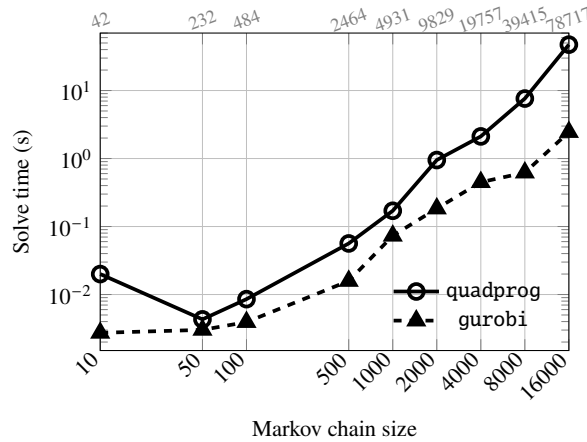


The whiskers extend to the most extreme data points that are not classified as outliers according to the standard 1.5 interquartile range criterion. Individual data points are overlaid as jittered dots, where each dot represents the outcome of a single test case. The horizontal jitter is introduced solely to avoid overlap and does not convey additional information.

In Figure 4, we compare the Frobenius norm of the perturbation Δ (i.e., the distance to reversibility, with sparsity constraints) obtained through our optimization procedure with the distance at which the Metropolis–Hastings reversibilization (Equations (6)–(7)) of the original matrix sits. We observe that the Metropolis–Hastings approach produces a reversible matrix that is further apart. In terms of algorithmic performance, the two optimization methods exhibit notable differences across the evaluated metrics. In terms of computational efficiency, `gurobi` emerges as the clear winner, achieving solve times approximately three to four times faster than `quadprog`, with median times around 0.007 s compared to `quadprog`’s 0.023 s. Concerning constraint satisfaction, the two solvers maintain excellent accuracy in enforcing the reversibility condition, with stationarity metrics showing negligible violations across all methods. However, the stochasticity constraint reveals a more pronounced difference: `gurobi` enforce this constraint with minimal violations at machine precision levels ($\sim 4.44 \times 10^{-16}$), while MATLAB’s `quadprog` method exhibits larger violations. Overall, `gurobi` provides the best results.

To assess the scalability of the proposed approach, we examine the computational time as a function of the problem size. Fig. 5 illustrates the solve time scaling behavior across test cases of varying dimensions. The horizontal axis represents the size of the Markov chain (i.e., the number of states), while the top axis indicates the number of nonzero entries in the original sparse transition matrix, reflecting the sparsity structure of each instance. The results reveal that both algorithms exhibit subquadratic scaling

Fig. 5 Solve time as a function of the Markov chain size (bottom axis) and the number of nonzero entries in the original sparse transition matrix (top axis). The two optimization algorithms demonstrate similar scaling behavior, with computational cost increasing with both the problem dimension and the sparsity level.



with respect to the problem size, which is favorable for large-scale applications. `gurobi` consistently outperforms MATLAB’s `quadprog` across all problem sizes, maintaining its computational advantage even as the dimension increases. The correlation between solve time and the number of nonzero entries underscores the importance of sparsity in the original transition matrix: denser matrices lead to more complex optimization problems with a larger number of active constraints, consequently requiring longer solution times. For small to moderately sized problems (up to approximately 100 states

with a few hundred nonzero entries), both methods deliver solutions in well under one second, demonstrating the viability of the approach for real-time or near-real-time applications in moderate-dimensional settings.

4.1.2 Comparison with the Riemannian approach for dense Markov Chains

To complete the benchmark, we compare Alg. 1—employing `gurobi`—with the Riemannian algorithm proposed in [11] for computing the nearest reversible matrix without structural constraints. In Fig. 6, the left panel displays the sparsity pattern of the transition matrix of the original Markov chain, which has size 251×251 with 1240 nonzero entries. The matrix is generated according to the same procedure described in Section 4.1.1. The

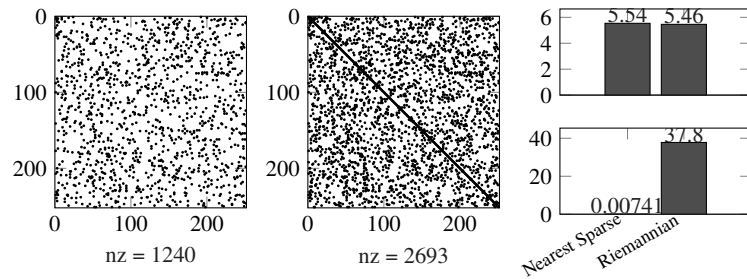


Fig. 6: Comparison with the Riemannian solver. *Left*: sparsity pattern of the transition matrix of the initial Markov chain. *Center*: sparsity pattern of the nearest sparse reversible transition matrix obtained with Alg. 1. *Right*: the Riemannian solver produces a dense matrix (not shown as a sparsity pattern). The top bar plot reports the perturbation norm, while the bottom bar plot shows the computational time required, respectively, by the approach here proposed (Sparse Nearest) and by the Riemannian solver.

central panel shows the sparsity pattern of the *nearest sparse reversible chain* computed with Alg. 1. The number of nonzero entries increases to 2693, which is comparable to the result reported in Fig. 2. By contrast, the Riemannian solver produces a dense matrix by construction.

We next compare the norm of the perturbations, reported in the top bar plot. The obtained values are approximately 5.54 for the *sparse* solver and 5.46 for the Riemannian solver. This ordering is expected, since the Riemannian approach allows modifications on all entries, thus enjoying greater flexibility. Nevertheless, restricting the admissible nonzero pattern does not significantly deteriorate the achieved norm.

Finally, we observe that the reduced number of nonzero entries makes the sparse solver substantially faster: it computes the solution in 7.41×10^{-2} seconds, compared to 37.8 seconds required by the Riemannian solver.

4.2 Direct estimation of Markov chains from transition counts

We consider a system governed by the Langevin stochastic differential equation [19]

$$\dot{x} = -\frac{\partial U(x)}{\partial x} + \xi(t), \quad x \in \mathbb{R}, \quad (17)$$

where $U(x)$ is a potential and $\xi(t)$ denotes Gaussian white noise with covariance $\langle \xi(t) \xi(s) \rangle = \sigma^2 \delta(t - s)$. For numerical simulations, the Euler–Maruyama scheme [18, 14] is employed, yielding

$$x(t + \Delta t) = x(t) - \frac{\partial U(x(t))}{\partial x} \Delta t + \sigma \sqrt{\Delta t} \eta(t), \quad (18)$$

with $\eta(t)$ independent standard Gaussian variables.

The resulting trajectory $\{x(t_n)\}_{n=0}^N$ is coarse-grained by partitioning the state space into B disjoint sets $\{\Theta_i\}_{i=1}^B$, which define the states of a Markov model. From the trajectory one forms the count matrix C , where C_{ij} denotes the number of transitions from Θ_i to Θ_j . The transition probability matrix P is then estimated via row normalization,

$$P_{ij} = \frac{C_{ij}}{\sum_{k=1}^B C_{ik}}, \quad P\mathbf{1} = \mathbf{1}.$$

Although the underlying Langevin dynamics are reversible, the finite-time discretization and sampling noise generally yield an estimator P that violates reversibility as seen in Definition 4. Reversibility is typically restored by post-processing, e.g., through reversibilization projections [5] or constrained optimization [11, 25].

4.2.1 An example of Markov chains constructed from the counting matrix

As a concrete example of the Langevin dynamics introduced in (17)–(18), we consider the torsional motion of the butane molecule, modeled by the potential

$$U(x) = a + b \cos(x) + c \cos^2(x) + d \cos^3(x),$$

which provides an effective approximation of the butane dihedral energy profile [25]. Here, x denotes the central dihedral angle, and the parameters are set to $a = 2.0567$, $b = -4.0567$, $c = 0.3133$, and $d = 6.4267$. Since $U(x)$ is periodic with period 2π , we restrict the state space to the interval $[0, 2\pi]$, which we partition into $B = 30$ disjoint subsets. The Langevin dynamics are then integrated using the Euler–Maruyama scheme (18), with step size $\Delta t = 10^{-3}$, noise intensity $\sigma = 1$, and total number of steps $N = 5 \times 10^8$. The resulting discrete trajectory is subsequently coarse-grained by the partition, yielding the state sequence used for the construction of the Markov model as described in the previous Section 4.2.

We generate a transition matrix P from the count matrix corresponding to this configuration and apply the proposed optimization strategy to recover a reversible

approximation. The resulting matrix P has no transient states and consists of a single ergodic class, so the reversible approximation can be computed directly on the full state space. We then compute the nearest reversible matrix according to our formulations employing the 'gurobi' QP algorithm and summarize the results in Fig. 7. The norm of the

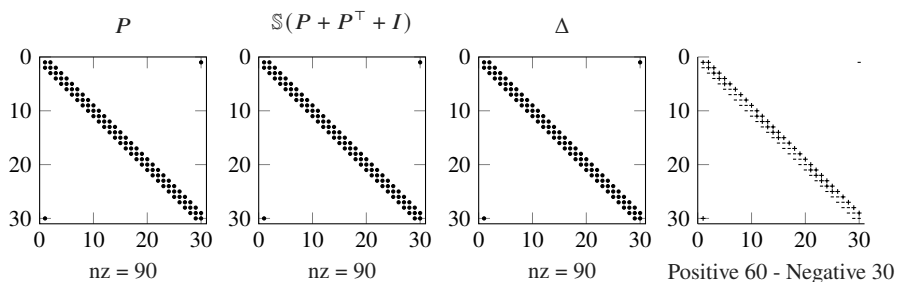


Fig. 7: Reversibilization of the transition matrix P obtained from the count matrix of the butane configuration. The four panels, from left to right, show: (i) the adjacency matrix of the original Markov chain P ; (ii) the admissible modification pattern $\mathbb{S}(P + P^\top + I)$; (iii) the sparsity pattern of the perturbation Δ obtained from the Nearest Sparse Reversible problem; (iv) the sign of the modification.

modification is $\|\Delta\|_F \approx 0.021858$, which is inferior to the norm of the perturbation with respect to the Metropolis–Hastings reversibilization in (6)-(7) which sits at a distance ≈ 0.057561 . Moreover, the constraint residuals satisfy $\|(P+\Delta)\mathbf{1}-\mathbf{1}\|_\infty \approx 2.2204 \times 10^{-16}$, $\|D_\pi(P+\Delta)-(P+\Delta)^\top D_\pi\|_\infty \approx 2.1684 \times 10^{-18}$, and $\|\pi^\top(P+\Delta)-\pi^\top\|_\infty \approx 5.5511 \times 10^{-17}$. These values indicate that the computed solution satisfies all constraints to machine precision. The modification redistributes the weights within the existing symmetric sparsity pattern. In particular, most diagonal entries and the lower first off-diagonal entries $(i, i-1)$ are increased (marked by “+”), whereas the upper first off-diagonal entries $(i, i+1)$ are predominantly decreased (marked by “-”). In addition, the corner entry $(1, 30)$ is increased, while its symmetric counterpart $(30, 1)$ is decreased. Overall, the sparsity pattern remains unchanged, but the mass is shifted from the upper diagonal toward the main and lower diagonals.

4.2.2 A more elaborate approach using a Markov State Model

We consider here a more elaborate construction than the simple estimate of the Markov chain obtained from the count matrix approach described in Section 4.2. As a test system, we considered a dataset [21] for Fs-peptide, a synthetic 21-residue peptide (Ace-A₅-(AAARA)₃-A-Nme) that is widely used as a minimal model for studying α -helical folding². Its relatively small size, combined with rich conformational dynamics

² Each trajectory in the simulated data for this protein system is 500 ns in length, and saved at a 50 ps time interval via 14 μ s aggregate sampling. The simulations were performed using the AMBER99SB-ILDN

on the nanosecond to microsecond timescale, makes it an ideal benchmark for evaluating kinetic models. The construction described below follows closely the Fs-peptide example provided in the MSMBuilder library³, which we reproduce here in order to illustrate how we arrive at a non-reversible Markov chain from the elaboration of a dynamical model.

The procedure consists of *featurization*, *dimensionality reduction*, *clustering*, and *estimation of the transition matrix*. First, the raw molecular dynamics trajectories, given as atomic coordinates $\{\mathbf{r}_t\}_{t=0}^T$, were transformed into an internal coordinate representation—i.e., a *featurizer* is used which transforms Cartesian coordinates into a most suitable coordinate systems. In particular, we extracted the set of backbone dihedral angles (ϕ, ψ) , producing a sequence of feature vectors $\mathbf{x}_t \in \mathbb{R}^d$, where d is the number of features; this reduces the space from the original 264×3 -dimensional space to $d = 84$ dimensions. Dihedral angles are then centered and scaled out by their respective interquartile ranges to reduce bias in the data.

Next, we applied time-structure independent component analysis (tICA) [20, 24] to identify the slow collective motions. Intuitively, tICA can be understood as a time-aware version of principal component analysis (PCA). While PCA finds directions of maximum variance, tICA finds directions along which the system evolves as slowly as possible, i.e., directions that maximize time-lagged correlations. In matrix terms, let $C_0 = \mathbb{E}[\mathbf{x}_t \mathbf{x}_t^T]$ be the covariance matrix and $C_\tau = \mathbb{E}[\mathbf{x}_t \mathbf{x}_{t+\tau}^T]$ the time-lagged covariance at lag time τ . The tICA components are obtained by solving the generalized eigenvalue problem

$$C_\tau \mathbf{w} = \lambda C_0 \mathbf{w},$$

where λ measures the autocorrelation of the signal projected along direction \mathbf{w} . The dominant eigenvectors $\{\mathbf{w}_i\}$ define linear projections $\mathbf{y}_t = W^T \mathbf{x}_t$ that emphasize the slowest modes of the peptide’s dynamics. In our application this reduces the number of dimensions from 84 to 4; Fig. 8a shows an histogram of the reduced data projected along the two slowest degrees of freedom as identified by the tICA. The reduced coordinates $\{\mathbf{y}_t\}$ were then discretized by clustering with MiniBatch k -Means [26]. Each MD frame was assigned to the nearest cluster center, producing a sequence of discrete microstate labels $s_t \in \{1, \dots, K\}$, where K is the number of clusters as depicted in Fig. 8b. From these microstate trajectories we estimated the transition probability matrix $P(\tau)$ at lag time τ by counting transitions:

$$P_{ij}(\tau) = \frac{C_{ij}(\tau)}{\sum_j C_{ij}(\tau)}, \quad P\mathbf{1} = \mathbf{1}, \quad (19)$$

where $C_{ij}(\tau)$ is the number of observed transitions from state i to j separated by τ time units.

We now apply the proposed optimization strategy to compute the nearest reversible transition matrix to the estimate P obtained from (19) using the procedure described above. The estimated matrix P consists of a single ergodic class and has no transient states;

force field with GBSA-OBC implicit solvent at 300K, starting from randomly sampled conformations from an initial 400K unfolding simulation. The simulation in the dataset have been run with the OpenMM (openmm.org) software.

³ See the example <http://msmbuilder.org/3.8.0/examples/Fs-Peptide-in-RAM.html>.

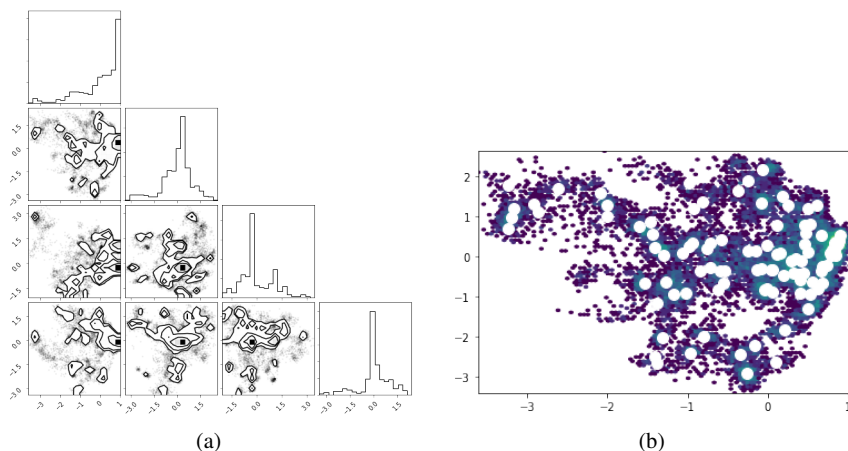


Fig. 8: Illustration of the MSM construction for the Fs-peptide system. Panel 8a reports the projection of the trajectories onto the first two tICA components, and is followed by panel 8b which gives discretization into clusters/microstates obtained by using MiniBatch k -Means [26]—cluster centers are represented as large white dots. These clusters serve as the discrete states on which the Markov State Model is estimated.

consequently, the optimization is performed over the full state space. The corresponding results are shown in Fig. 9.

The perturbation modifies all entries permitted by the admissible pattern, resulting in $\text{nnz}(\Delta) = 918$. The Frobenius norm of Δ is approximately 0.134822, which is approximately five times smaller than the distance ≈ 0.653852 achieved by the Metropolis-Hastings reversibilization (6)-(7). The optimization was carried out using the 'gurobi' solver option, with solution times of 0.0036 s. The constraint residuals satisfy $\|(P + \Delta)\mathbf{1} - \mathbf{1}\|_\infty \approx 4.440892 \times 10^{-16}$, $\|D_\pi(P + \Delta) - (P + \Delta)^\top D_\pi\|_\infty \approx 2.775558 \times 10^{-17}$, and $\|\pi^\top(P + \Delta) - \pi^\top\|_\infty \approx 1.396265 \times 10^{-17}$.

5 Conclusions

In this work, we have developed a comprehensive optimization framework for computing the nearest reversible sparse Markov chain to a given non-reversible matrix. The reversibility constraint is expressed through the symmetry condition with respect to the stationary distribution, and we have embedded this constraint into the optimization problem. A key theoretical contribution is the proof that the underlying optimization problem is strongly convex, ensuring the existence and uniqueness of the solution and, crucially, its independence from the choice of optimization algorithm. This theoretical property provides robustness and consistency across different computational approaches. Through comparative analysis, we evaluated two state-of-the-art optimization algorithms—quadprog and gurobi—demonstrating their practical viability for

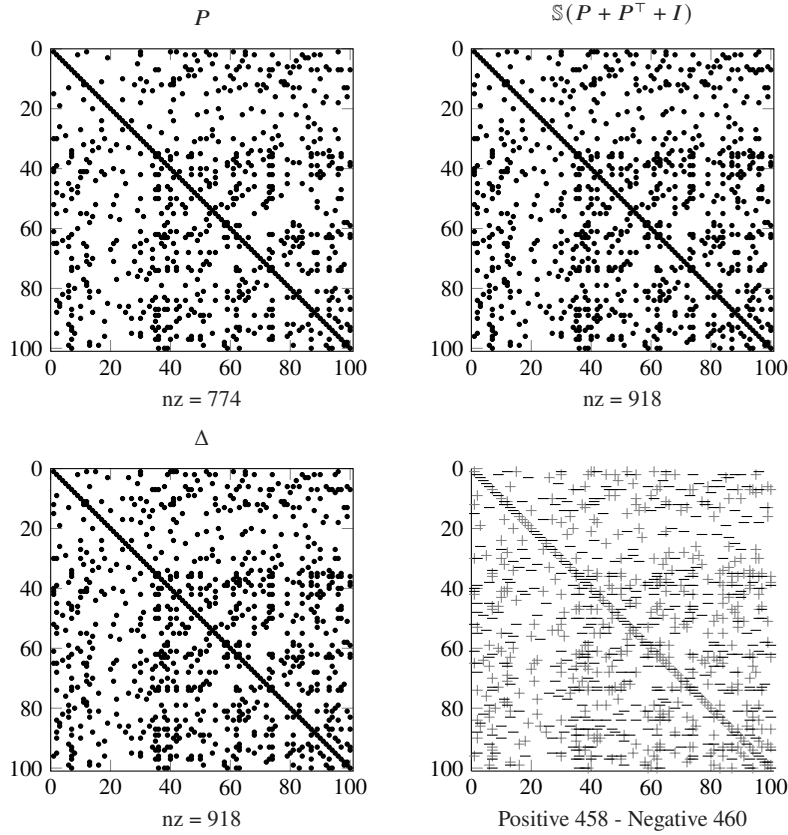


Fig. 9: Reversibilization of the transition matrix P from (19). The four panels, from left to right, show: (i) the sparsity pattern of the original matrix P , which is not symmetric; (ii) the admissible modification pattern $\mathbb{S}(P + P^\top + I)$; (iii) the sparsity pattern of the perturbation Δ ; (iv) sign of the obtained Δ matrix.

both small and moderate-scale problems. Our experiments reveal that `gurobi` provides superior computational performance, achieving solve times approximately 3–4 times faster than `guadprog`, while all methods satisfy the reversibility and stationarity constraints to machine precision. The subquadratic scaling of computational cost with problem dimension underscores the scalability of the approach.

Extensive numerical experiments on synthetic sparse matrices and real-world examples from molecular dynamics simulations validate the proposed methodology. The results demonstrate that reversibility introduces a systematic and quantifiable increase in sparsity, an intrinsic consequence of the coupling constraints between forward and backward transitions. This fundamental trade-off is independent of the specific problem instance and algorithmic choice, suggesting that the sparsity-reversibility relationship reflects a deep structural property of Markov chains. Furthermore, the framework suc-

cessfully processes transition matrices obtained from empirical data (transition counts) and recovers reversible matrices with high constraint satisfaction. We plan to evaluate the usage of regularized interior point methods from [6, 7], to further accelerate the solution and increase the robustness of the method.

Acknowledgements This work was partially supported by the Italian Ministry of University and Research (MUR) through the PRIN 2022 “Low-rank Structures and Numerical Methods in Matrix and Tensor Computations and their Application” code: 20227PCCKZ MUR D.D. financing decree n. 104 of February 2nd, 2022 (CUP I53D23002280006) and through the PRIN 2022 “MOLE: Manifold constrained Optimization and LEarning”, code: 2022ZK5ME7 MUR D.D. financing decree n. 20428 of November 6th, 2024 (CUP B53C24006410006). The last three authors are member of the INdAM GNCS and acknowledge the MUR Excellence Department Project awarded to the Department of Mathematics, University of Pisa, CUP I57G22000700001. Furthermore, during part of the preparation of this work, MG was affiliated with the Department of Mathematics, University of Pisa, Pisa (Italy).

Competing Interests The authors have no conflicts of interest to declare that are relevant to the content of this chapter.

References

1. Altman, A., Gondzio, J.: Regularized symmetric indefinite systems in interior point methods for linear and quadratic optimization. *Optim. Methods Softw.* **11/12**(1-4), 275–302 (1999). DOI 10.1080/10556789908805754. URL <https://doi.org/10.1080/10556789908805754>. Interior point methods
2. Barker, A.A.: Monte Carlo Calculations of the Radial Distribution Functions for a Proton-Electron Plasma. *Australian Journal of Physics* **18**(2), 119–134 (1965). DOI 10.1071/PH650119. URL <https://doi.org/10.1071/PH650119>
3. Berman, A., Plemmons, R.J.: Nonnegative matrices in the mathematical sciences, *Classics in Applied Mathematics*, vol. 9. Society for Industrial and Applied Mathematics (SIAM), Philadelphia, PA (1994). DOI 10.1137/1.9781611971262. URL <https://doi.org/10.1137/1.9781611971262>. Revised reprint of the 1979 original
4. Boumal, N.: An introduction to optimization on smooth manifolds. Cambridge University Press, Cambridge (2023)
5. Choi, M.C.H., Wolfer, G.: Systematic Approaches to Generate Reversibilizations of Markov Chains. *IEEE Transactions on Information Theory* **70**(5), 3145–3161 (2024). DOI 10.1109/TIT.2023.3304685
6. Cipolla, S., Gondzio, J.: Proximal stabilized interior point methods and *low-frequency-update* preconditioning techniques. *J. Optim. Theory Appl.* **197**(3), 1061–1103 (2023). DOI 10.1007/s10957-023-02194-4. URL <https://doi.org/10.1007/s10957-023-02194-4>
7. Cipolla, S., Gondzio, J., Zanetti, F.: A regularized interior point method for sparse optimal transport on graphs. *European J. Oper. Res.* **319**(2), 413–426 (2024). DOI 10.1016/j.ejor.2023.11.027. URL <https://doi.org/10.1016/j.ejor.2023.11.027>
8. Diestel, R.: Graph theory, *Graduate Texts in Mathematics*, vol. 173, sixth edn. Springer, Berlin (2025)
9. Douik, A., Hassibi, B.: Manifold Optimization Over the Set of Doubly Stochastic Matrices: A Second-Order Geometry. *IEEE Transactions on Signal Processing* **67**(22), 5761–5774 (2019). DOI 10.1109/TSP.2019.2946024
10. Durastante, F., Gnazzo, M., Meini, B.: Kemeny’s constant minimization for reversible Markov chains via structure-preserving perturbations (2025). URL <https://arxiv.org/abs/2510.24679>

11. Durastante, F., Gnazzo, M., Meini, B.: A Riemannian Optimization Approach for Finding the Nearest Reversible Markov Chain (2025). URL <https://arxiv.org/abs/2505.16762>
12. Gilks, W.R., Richardson, S., Spiegelhalter, D.J. (eds.): Markov chain Monte Carlo in practice. Interdisciplinary Statistics. Chapman & Hall, London (1996). DOI 10.1007/978-1-4899-4485-6. URL <https://doi.org/10.1007/978-1-4899-4485-6>
13. Hastings, W.K.: Monte Carlo sampling methods using Markov chains and their applications. *Biometrika* **57**(1), 97–109 (1970). DOI 10.1093/biomet/57.1.97. URL <https://doi.org/10.1093/biomet/57.1.97>
14. Higham, D.J.: An algorithmic introduction to numerical simulation of stochastic differential equations. *SIAM Rev.* **43**(3), 525–546 (2001). DOI 10.1137/S0036144500378302. URL <https://doi.org/10.1137/S0036144500378302>
15. Higham, N.J.: Matrix nearness problems and applications. In: Applications of matrix theory (Bradford, 1988), *Inst. Math. Appl. Conf. Ser. New Ser.*, vol. 22, pp. 1–27. Oxford Univ. Press, New York (1989). DOI 10.1093/imamat/22.1.1. URL <https://doi.org/10.1093/imamat/22.1.1>
16. Kelly, F.P.: Reversibility and stochastic networks. Wiley Series in Probability and Mathematical Statistics. John Wiley & Sons, Ltd., Chichester (1979)
17. Kemeny, J.G., Snell, J.L.: Finite Markov chains. Undergraduate Texts in Mathematics. Springer-Verlag, New York-Heidelberg (1976). Reprinting of the 1960 original
18. Kloeden, P.E., Platen, E.: Stochastic Differential Equations, pp. 103–160. Springer Berlin Heidelberg, Berlin, Heidelberg (1992). DOI 10.1007/978-3-662-12616-5_4. URL https://doi.org/10.1007/978-3-662-12616-5_4
19. Kürsten, R., Behn, U.: Patchwork sampling of stochastic differential equations. *Phys. Rev. E* **93**, 033307 (2016). DOI 10.1103/PhysRevE.93.033307. URL <https://link.aps.org/doi/10.1103/PhysRevE.93.033307>
20. M. Sultan, M., Pande, V.S.: tICA-Metadynamics: Accelerating Metadynamics by Using Kinetically Selected Collective Variables. *Journal of Chemical Theory and Computation* **13**(6), 2440–2447 (2017). DOI 10.1021/acs.jctc.7b00182. URL <https://doi.org/10.1021/acs.jctc.7b00182>. PMID: 28383914
21. McGibbon, R.T.: Fs MD Trajectories (2014). DOI 10.6084/m9.figshare.1030363.v1. URL https://figshare.com/articles/dataset/Fs_MD_Trajectories/1030363
22. Metropolis, N., Rosenbluth, A.W., Rosenbluth, M.N., Teller, A.H., Teller, E.: Equation of State Calculations by Fast Computing Machines. *The Journal of Chemical Physics* **21**(6), 1087–1092 (1953). DOI 10.1063/1.1699114. URL <https://doi.org/10.1063/1.1699114>
23. Meyer, C.: Matrix analysis and applied linear algebra. Society for Industrial and Applied Mathematics (SIAM), Philadelphia, PA (2000). DOI 10.1137/1.9780898719512. URL <https://doi.org/10.1137/1.9780898719512>. With 1 CD-ROM (Windows, Macintosh and UNIX) and a solutions manual (iv+171 pp.)
24. Molgedey, L., Schuster, H.G.: Separation of a mixture of independent signals using time delayed correlations. *Phys. Rev. Lett.* **72**, 3634–3637 (1994). DOI 10.1103/PhysRevLett.72.3634. URL <https://link.aps.org/doi/10.1103/PhysRevLett.72.3634>
25. Nielsen, A.J.N., Weber, M.: Computing the nearest reversible Markov chain. *Numer. Linear Algebra Appl.* **22**(3), 483–499 (2015). DOI 10.1002/nla.1967. URL <https://doi.org/10.1002/nla.1967>
26. Sculley, D.: Web-scale k-means clustering. In: Proceedings of the 19th International Conference on World Wide Web, WWW '10, p. 1177–1178. Association for Computing Machinery, New York, NY, USA (2010). DOI 10.1145/1772690.1772862. URL <https://doi.org/10.1145/1772690.1772862>
27. Tarjan, R.: Depth-first search and linear graph algorithms. *SIAM J. Comput.* **1**(2), 146–160 (1972). DOI 10.1137/0201010. URL <https://doi.org/10.1137/0201010>
28. Trendelkamp-Schroer, B., Wu, H., Paul, F., Noé, F.: Estimation and uncertainty of reversible Markov models. *The Journal of Chemical Physics* **143**(17), 174101 (2015). DOI 10.1063/1.4934536. URL <https://doi.org/10.1063/1.4934536>
29. Wolfer, G., Watanabe, S.: Information Geometry of Reversible Markov Chains. *Information Geometry* **4**(2), 393 – 433 (2021). DOI 10.1007/s41884-021-00061-7